Acta Technica *62* (2017), No. 4A, 457–464

Numerical calculation of particle diameter effect inside a two phases flow sewage pump

Junjian Xiao[2], Yuliang Zhang[2], Yanjuan Zhao[3]

Abstract. Based on Mixture model and SIMPLE algorithm, we performed a numerical calculation on the internal flow field when solid–liquid two-phase flow is conveyed though sewage pump. In addition, we analyzed the influence of the diameter of solid particles on the hydraulic performance of sewage pump and the prediction on the degree of blade wear. Results show that with the enlargement of particle diameter, the head and efficiency of pump decrease monotonously, and the shaft power shows a trend of decreasing first and then increasing. The total pressure on the blade pressure surface tends to decrease gradually. The solid-phase concentration on the blade pressure surface shows a gradual decline. The position points with the same total pressures as pressure and suction surfaces move forward. The shaft power has a minimum value for some particle diameter.

Key words. sewage pump, solid diameter, numerical calculation, abrasion.

1. Introduction

A sewage pump is a solid–liquid two-phase flow pump and is used as the key equipment in urban river dredging. Many scholars at home and abroad have conducted in-depth research and achieved fruitful results. Engin et al. considered a semi-open impeller centrifugal pump as research object, compared the pump performance when the pump conveyed water, sand, and other hard materials, and developed an equation that expresses the effect of particle size on pump performance; the deviation between the predicted value and the measured value of the solid–liquid two-phase pump head was between ?20% and +15% [1]. Gandhi et al. studied the

[1]Acknowledgement - The work was supported by the Zhejiang Provincial Natural Science Foundation of China (No.LY18E090007), Academic Foundation of Quzhou University (No.XNZQN201508), and Chinese National Foundation of Natural Science (No.51536008).

[2]College of Mechanical Engineering, Quzhou University, Quzhou 324000, China

[3]College of Information Engineering, Quzhou College of Technology, Quzhou 324000, China

performance of a closed impeller centrifugal pump for conveying water, mortar, and zinc tailings with solid–liquid mixed media[2]. Yuan et al. conducted a numerical simulation study on solid–liquid two-phase turbulence inside a non-overload mud [3] and found a reflux in the inlet and a velocity slip between the two phases. Li et al. performed an experiment on the effect of solid particle properties (including concentration and particle size) on the external characteristics of centrifugal pump [4]. Zhang et al. adopted a numerical calculation method for a numerical study on solid–liquid two-phase flow field in a low-specific-speed centrifugal pump [5] and found a clear jet-wake structure near the volute tongue that became apparent as the volume fraction increased. Zhang et al. performed a numerical simulation on the initial characteristics when a high-specific-speed centrifugal pump conveyed solid–liquid two-phase flow [6]. Harry et al. studied a centrifugal pump blade made of high-chrome white iron and aluminum alloy through Coriolis experiment [7] and obtained different wear forms of the centrifugal pump blade when the mud was conveyed.

Considering that many designs are developed from experience, pump performance is not guaranteed. Therefore, the internal flow of pump needs to be studied to establish a theoretical basis for designing a pump with high performance and stable operation. This research performs numerical simulation and analysis on a solid–liquid two-phase flow pump and analyzes the effect of the diameter of solid particles on the performance of the sewage pump. The internal pressure and the dynamic distribution of solid particles on the solid surface are also investigated.

2. Pump model and calculation method

2.1. Pump model and calculation mesh

The pump model is a medium-speed centrifugal pump with a specific speed ns = 129.3. The basic performance parameters of the pump are as follows: flow Q = 50 m3/h, head H = 20.54 m, speed n = 2900 r/min, shaft power Pa = 3.54 kW, efficiency η = 79.5%, NPSHC = 2.59 m. The main geometric dimensions of the pump include the following: diameter of pump inlet Dj = 76 mm, hub diameter dh = 0 mm, diameter of impeller outlet D2 = 137 mm, width of impeller outlet b2 = 14 mm, angle of blade outlet β2 = 30?, number of blade Z = 6, wrap angle φ = 104.5?, diameter of volute base D3 = 145 mm, width of volute inlet b3 = 30 mm.

2.2. Calculation mesh

The commercial software UG is used for the 3D modeling of the internal calculation domain. A proper extension is made for the straight pipe-type suction chamber to eliminate the influence of the given speed of the inlet. The same is true for the convergence calculation; the pump outlet is also extended. The mesh is divided in the calculation domain by the commercial meshing software GAMBIT2.3.16, as shown in Fig. 1. The tetrahedral mesh is used in the impeller rotation zone and the volute still zone; the numbers of the mesh are 435530 and 597127, respectively.

The hexahedral mesh is used in the extension section of the suction chamber; the numbers of the mesh are 152827 and 54944. The total number of the mesh in the computing domain is 1240428. The number of mesh is not adequate for the fine flow in the simulated boundary layer but sufficient for simulating the macro-flow of the pump and capturing the macroscopic characteristics of the pump. Mesh quality inspection reveals that the equiangular slope and the equal slope are not more than 0.83, the near wall Y + is approximately 30, and the mesh is of good quality.

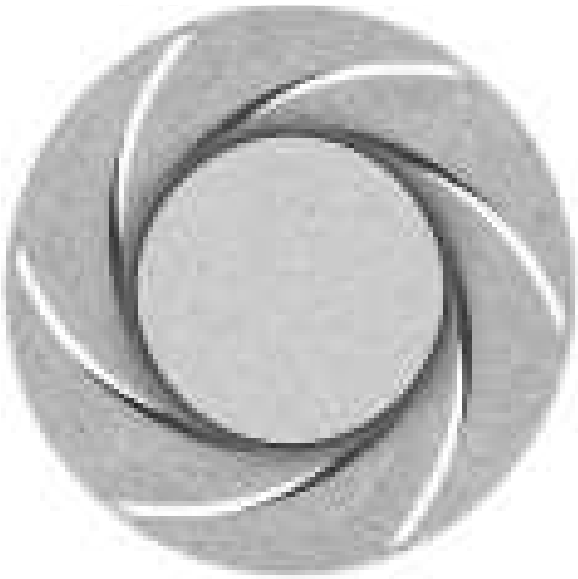

Fig. 1. Calculation mesh

2.3. Multiphase flow model

The RNG k-ε two-equation model is used in the unsteady turbulence calculation to make the Renault mean equation closed. In this study, 3D turbulent flow calculation of incompressible viscous fluid is conducted through business code-FLUENT software based on finite volume method. The algebraic slip mixture model (ASMM) [8] based on Euler–Euler method is used to calculate the solid–liquid two-phase flow in the numerical calculation of multiphase flow model. The particle equivalent is taken as quasi-fluid. In this study, the calculated medium is a solid–liquid two-phase flow. If a steady flow calculation is to be conducted, the phase of the local change rate will no longer exist in the above equation.

2.4. Solution settings

The dynamic and static coupling is realized by the "frozen rotor method." The velocity inlet and free discharge are used as boundary conditions for the inlet and outlet, respectively. The coupling between velocity and pressure is calculated through

SIMPLE algorithm. The spatial discretization of convective term adopts the first-order upwind scheme. The spatial discretization of diffusion term adopts the central difference scheme with second-order accuracy. The spatial discretization of source term adopts the linearized standard format. The solid particles are uniform spherical particles with the same physical properties. The convergence criterion for each control equation is 0.0001.

2.5. Calculation program

To explore the effect of solid-phase properties on the hydraulic conveying performance when the solid–liquid two-phase flow is conveyed by the sewage pump, the following calculation scheme is formulated: with the design discharge ($Q = 50$ m^3/h). The solid concentration is 10%, the density is 2500 kg/m^3, the diameters of particles are 0.01, 0.05, 0.10, 0.15, and 0.20 mm, and the solid–liquid two-phase flow field is numerically calculated.

3. Results analysis

3.1. External characteristics

The inlet and outlet pressures and the external characteristics of the pump obtained by numerical calculation based on the five particle diameters are shown in Figs. 2 and 3. Fig. 2 presents that when the particle diameters in the solid–liquid two-phase flow are 0.01, 0.05, 0.10, 0.15, and 0.20 mm, the total pressures at the pump inlet are 0.343, 0.348, 0.358, 0.386, and 0.413 kPa, and the total pressures at the pump outlet are 159.946, 156.559, 153.524, 151.882, and 149.709 kPa, respectively. With the enlargement of particle diameter, the total pressures of the pump inlet and outlet increase gradually, and the total pressure at the pump outlet drops more sharply.

The calculated result of external characteristics in Fig. 3 shows that when the particle diameters are 0.01, 0.05, 0.10, 0.15, and 0.20 mm, the heads are 14.38, 14.08, 13.81, 13.67, and 13.48 m, the efficiencies are 49.48%, 48.56%, 47.49%, 46.78%, and 45.95%, and the shaft powers are 4.549, 4.538, 4.551, 4.574, and 4.592 kW, respectively. With the enlargement of particle diameter, the head and the efficiency decrease monotonously, and the shaft power shows a trend of decreasing first and then increasing. The shaft power is the lowest when the particle diameter is 0.05 mm.

3.2. Characteristics of pressure surface

Fig. 4 shows the distribution of individual physical quantity on the pressure surface. The total pressure distribution of the pressure surface in Fig. 4 implies that the total pressure on the blade pressure surface tends to decrease gradually as the particle diameter enlarges. When the particle diameters are 0.01, 0.05, 0.10, 0.15, and 0.20 mm, if the relative length is 0.2, the total pressures of the blade

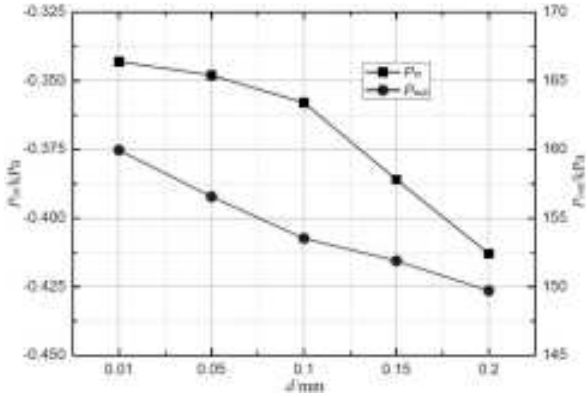

Fig. 2. Effect of particle diameter on the inlet and outlet pressures

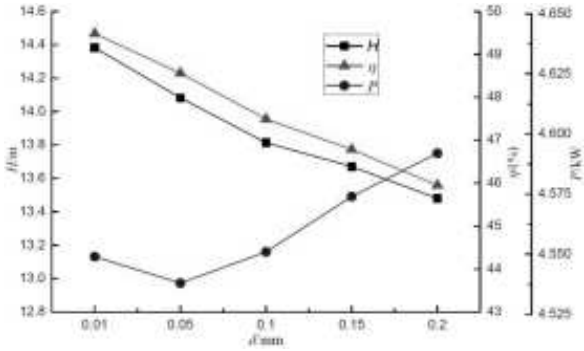

Fig. 3. External characteristics

pressure surface are 103.597, 97.593, 92.035, 88.118, and 85.263 kPa, respectively; if the relative length is 0.5, the total pressures of the blade pressure surface are 187.795, 176.663, 167.6, 162.431, and 160.145 kPa, respectively; if the relative length is 0.8, the total pressures of the blade pressure surface are 227.78, 218.427, 209.571, 203.885, and 200.085 kPa, respectively. The variation characteristics are consistent with those of the head curve. With an increase in the relative length, the total pressures of the blade pressure surface show a gradual upward trend, which is related to the performance of the blade, i.e., a large radius leads to a fast peripheral speed and great working capacity. The pressure drops sharply at the outlet of the blade pressure surface, which is caused by jet-wake effect.

The solid particles moving with the impeller at a high speed will produce varying degrees of wear on over-current components because the "sedimentation" of solid particles in the pump is a dynamic equilibrium deposition. Therefore, the numerical simulation on the position and principle of deposition of solid particles in the pump will reflect the degree of wear of over-current components, which will provide guidance for the design. The solid-phase concentration distribution of the blade pressure surface obtained through numerical calculation is clearly shown in Fig. 4 . As the particle diameter enlarges, the solid concentration of the blade pressure

surface decreases gradually. The larger the particle diameter is, the greater the mass of a single particle is, the greater the centrifugal force is, and the easier the particle detaches from the wall. Therefore, in this model, the wear on the blade pressure surface will be weakened as the particle diameter enlarges. Beyond that, the effect of particle size on the concentration distribution of the solid phase is not apparent at the front edge of the pressure surface; the calculated concentration is approximately 10%. When the particle diameter is 0.01 mm, the solid-phase concentration on the blade pressure surface is maintained at approximately 10%. The reason for this condition is that the particles are too small. If the particle diameters are 0.05, 0.10, 0.15, and 0.20 mm, the solid concentration decreases from the front edge as the relative length increases, and the reduction of dynamically changing concentration will be helpful to reduce the wear on the blade pressure surface. At the blade pressure surface outlet, the solid-phase concentrations are 9.823%, 8.31%, 6.908%, 5.799%, and 4.727% when the relative length is 1.

Fig. 4 shows that the effect of particle diameter on the pressure surface vorticity of the blade is insignificant. The calculation results indicate that the calculation range of vorticity significantly changes only when the particle diameter is 0.20 mm and the relative length is between 0.46 and 0.57. The absolute value of vorticity is minimum (only 1,841 $s^{?1}$) when the relative length is 0.5.

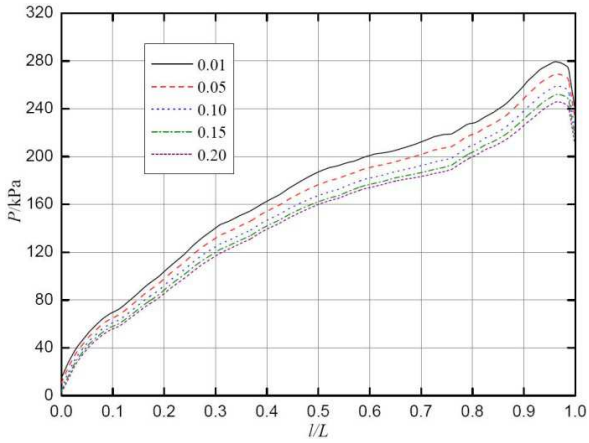

Fig. 4. Effect of particle diameter on the performance parameters of blade pressure surface

3.3. Characteristics of suction surface

Fig. 5 shows the distribution of physical quantities on the suction surface. The total pressure distribution in Fig. 5 implies that the change in particle diameter is not evident at the first half of the blade. For example, when the relative length is 0.1 and the particle diameters are 0.01, 0.05, 0.10, 0.15, and 0.20 mm, the total pressures are ?8.444, ?8.685, ?9.021, ?9.193, and ?9.687 kPa, respectively. The difference in the five total pressures is minimal. When the relative length is 0.5, the total pressures

are 76.229, 74.649, 73.698, 73.903, and 72.373 kPa. The difference in the five total pressures is also minimal. In the second half of the blade suction surface, with the enlargement of particle diameter, the total pressure shows a gradual increase as a whole. At the front edge of the blade suction surface, the total pressures are ?40.113, ?38.176, ?35.976, ?34.000, and ?32.751 kPa. At the rear edge of the blade suction surface, the total pressures are 293.892, 304.523, 323.675, 334.012, and 338.0881 kPa. Regardless of the solid particle diameter, the total pressure increases as the blade radius enlarges.

Fig. 5 illustrates the change in solid concentration on the blade suction surface. When the particle diameter is 0.01 mm, the solid-phase concentration on the blade suction surface is almost unchanged, and it is approximately 10%. The reason is that the particles are too small; the subsequent performance of particles following the water flow is good. In the case of solid particles with diameters of 0.05, 0.10, 0.15, and 0.20 mm, the change in the first half of the blade suction surface is minimal, but that in the second half is apparent. The four concentrations at the front edge are 9.532%, 9.374%, 9.508%, and 9.686%. The four concentrations in the middle are 10.824%, 12.236%, 13.628%, and 14.315%. The four concentrations at the rear edge are 14.161%, 21.022%, 25.107%, and 27.423%. In the second half of the blade suction surface, the solid-phase concentration tends to increase as the diameter of solid particles enlarges; the solid concentrations are 10.448%, 17.537%, 32.351%, 43.327%, and 49.52% when the relative length is 0.8.

Fig. 5 depicts the change in vortex on the blade suction surface. The effect of the diameter of solid particles on vorticity is insignificant. However, for any particle diameter, the vorticity of the blade suction surface changes slightly from the front edge.

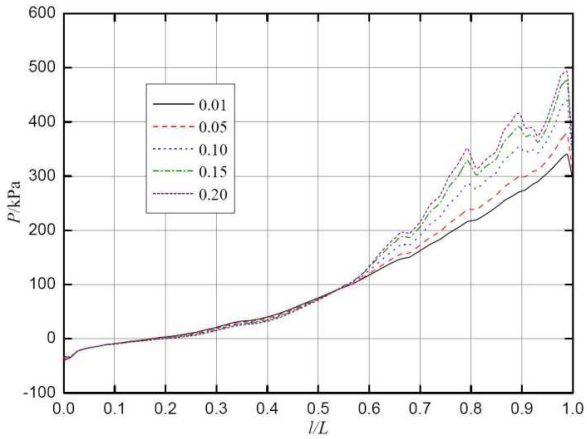

Fig. 5. Effect of particle diameter on the performance parameters of the blade suction surface

4. Conclusions

Results show that with an increase in particle diameter, the head and efficiency of the pump decrease monotonously, and the shaft power shows a trend of decreasing first and then increasing. The total pressure on the blade pressure surface tends to decrease gradually. The solid-phase concentration on the blade pressure surface shows a trend of gradual decline, and the position point with the same total pressure value on the pressure surface and the suction surface moves forward. The shaft power has a minimum value for some particle diameters.

References

[1] T. Engin, M. Gur: *Performance characteristics of centrifugal pump impeller with running tip clearance pumping solid-liquid mixtures.* Journal of Fluids Engineering *123* (2001), No. 3, 532–538.

[2] B. K. Gandhi, S. N. Singh, V. Seshadn: *Effect of speed on the performance characteristics of a centrifugal slurry pump.* Journal of Hydraulic Engineering *128* (2002), No. 2, 225–233.

[3] S. Q. Yuan, P. F. Zhang, J. F. Zhang: *Numerical simulation of 3-D dense solid-liquid two- phase turbulent flow in a non-clogging mud pump.* Chinese Journal of Mechanical Engineering *17* (2004), No. 4, 623–627.

[4] L. Yi, Z. C. Zhu, W. Q. He: *Numerical simulation and experimental research on the influence of solid phase characteristics on centrifugal pump performance.* Chinese Journal of Mechanical Engineering *25* (2012), No. 6, 1184–1189.

[5] Y. L. Zhang, L. Yi, B. L. Cui: *Numerical simulation and analysis of solid-liquid two-phase flow in centrifugal pump.* Chinese Journal of Mechanical Engineering *26* (2013), No. 1, 53–60.

[6] Y. L. Zhang, L. Yi, Z. C. Zhu: *Computational analysis of centrifugal pump delivering solid-liquid two-phase flow during startup period.* Chinese Journal of Mechanical Engineering *27* (2014), No. 1, 178–185.

[7] H. T. Harry, R. A. Graeme: *Experimental study on erosive wear of some metallic materials using Coriolis wear testing approach.* Wear (2005), No. 258, 458–469.

[8] J. Sanyal, S. Vasquez, S. Roy: *Numerical simulation of gas-liquid dynamics in cylindrical bubble column reactors.* Chemical Engineering Science *54* (1999), No. 21, 5071–5083.

Received November 16, 2016